Supplementary Figure 1

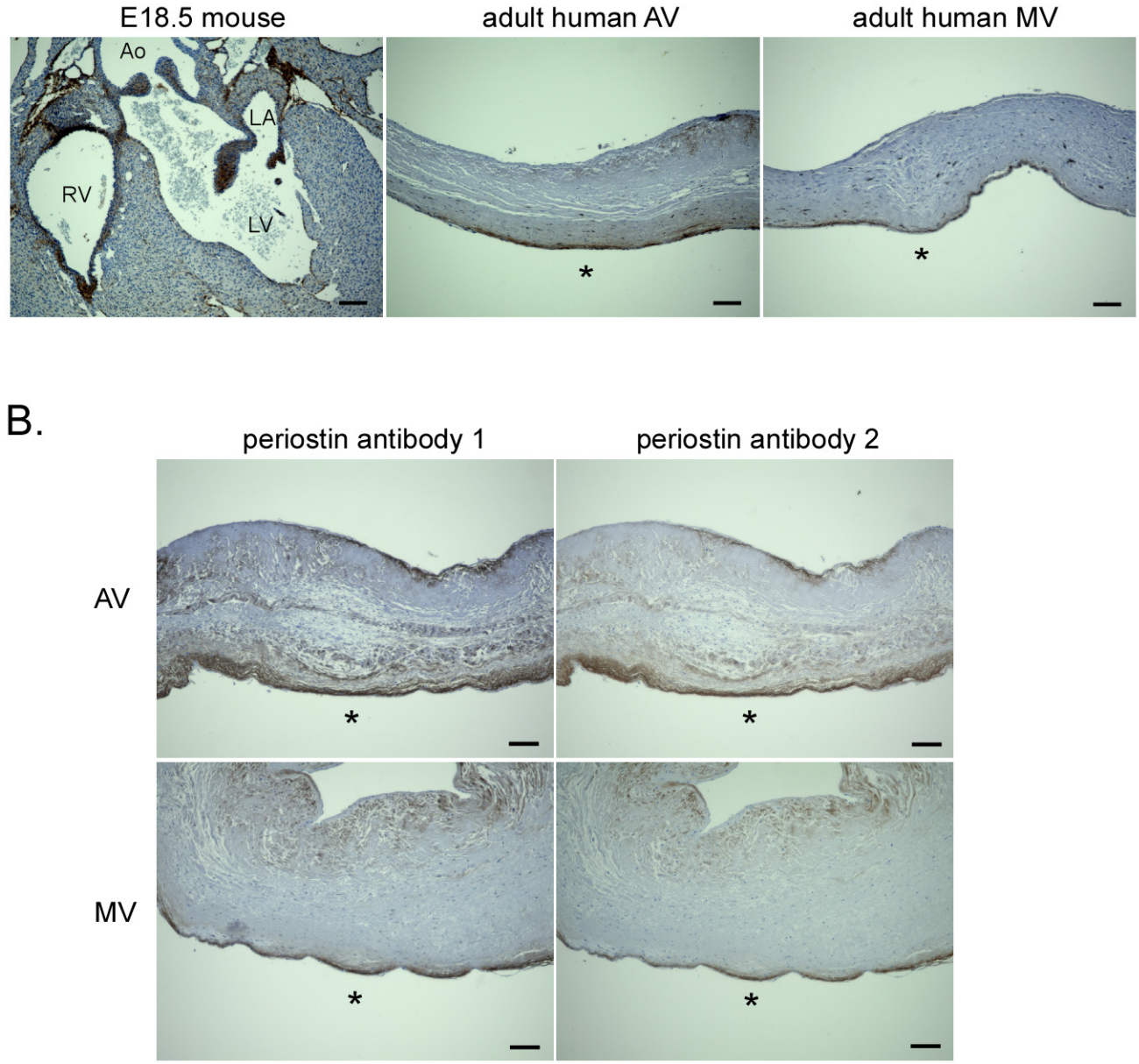

Physiologic expression patterns of periostin in embryonic mouse and adult human cardiac valves. (A) Representative IHC sections (stained with the periostin antibody used in Figure 2) of E18.5 murine valves and the cardiac valves of an autopsied 69-yr-old patient. (B) IHC sections of the aortic and mitral valves from the 45-yr-old and 68 yr-old patients shown in Figure 2, respectively, using different periostin antibodies. Note that periostin is expressed throughout the cardiac valves of the mouse embryo, whereas its expression is localized in the normal valves of the adult human. Asterisks denote the ventricularis and atrialis sides of the aortic and mitral valves, respectively. Scale bars: 100 μm.

Supplementary Figure 2

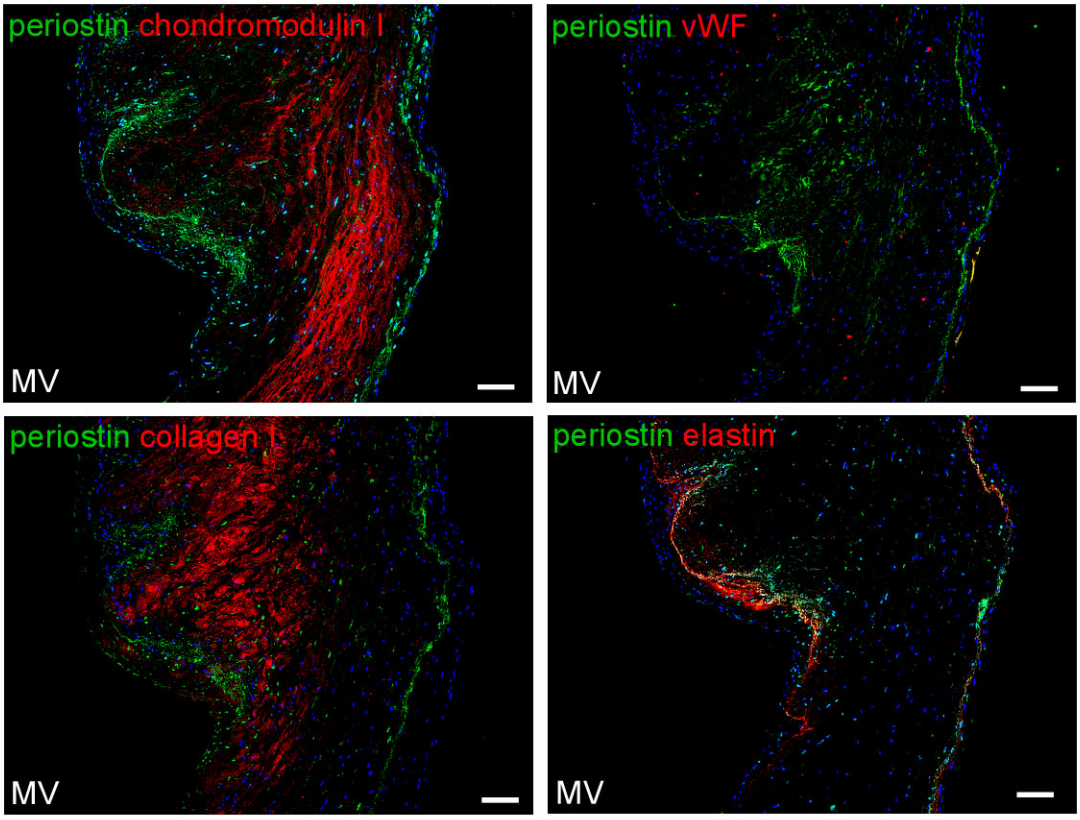

Periostin localization in adult human normal mitral valves. Representative, consecutive sections of normal mitral valves were subjected to triple-immunofluorescence staining. Scale bars: 100 μm.

Supplementary Figure 3

Expression of periostin and other components in normal mitral valves and VHD valves. Representative, consecutive IHC sections of normal human mitral valves, rheumatic MR, and MV prolapse are shown. The boxed regions are shown at higher magnification in the insets. Note that the areas of expression of periostin, vWF, VEGF, and α-SMA are expanded, while that of chondromodulin I is reduced in rheumatic MR, but not in MV prolapse. Scale bars: 500 μm (100 μm for the higher magnification).

Supplementary Figure 4

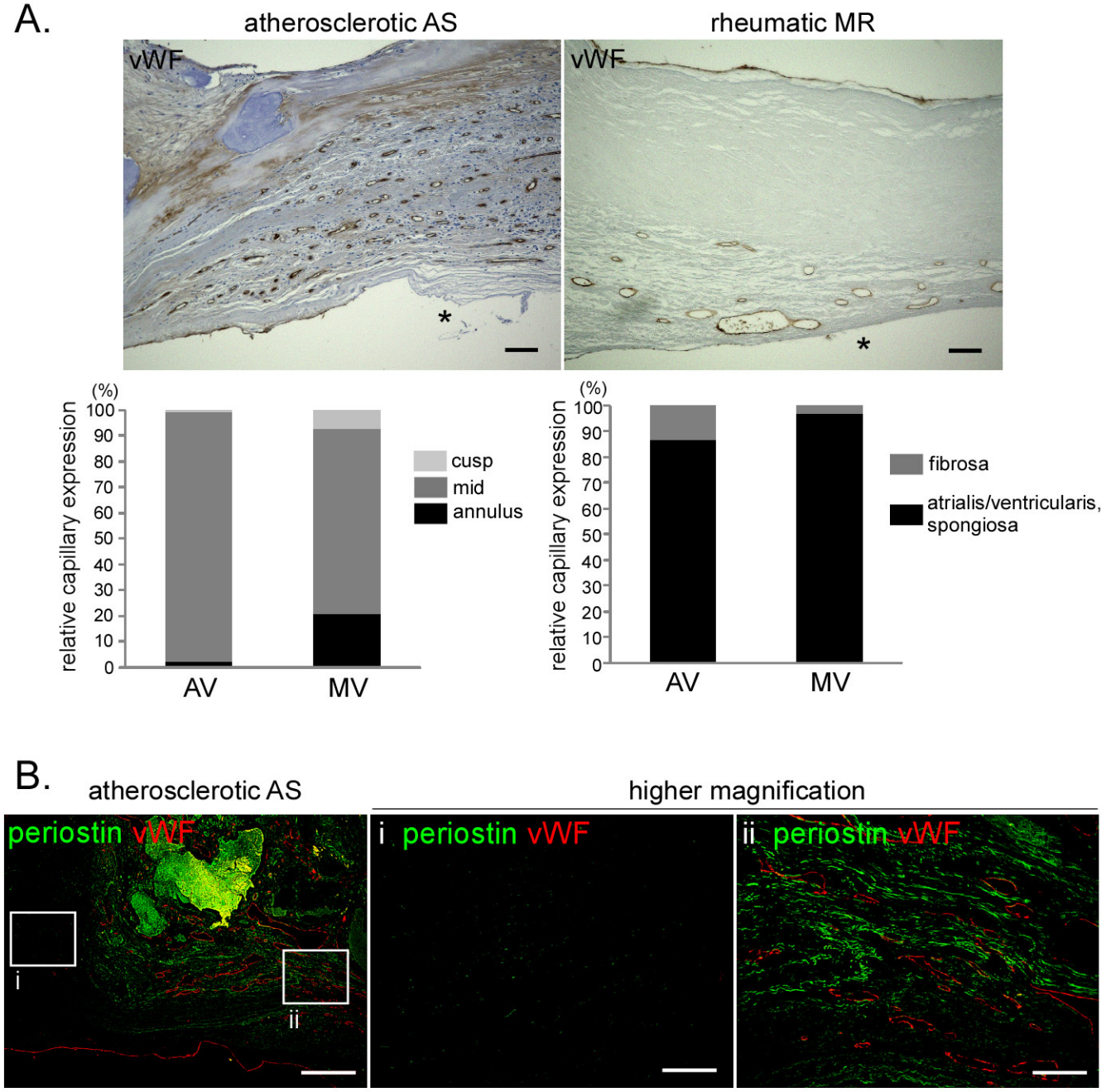

The areas of angiogenesis and periostin expression in human VHD. (**A**) Representative IHC staining for vWF of sections of human atherosclerotic aortic valve stenosis and rheumatic mitral regurgitation are shown. Note that neoangiogenesis is mainly detected in the zona atrialis/ventricularis and zona spongiosa within the valves, where vWF expression is diminished in the valve endocardium (asterisks). The graphs show the relative expression levels of the capillaries in each region of the valves of VHD. AS, aortic valve stenosis; MR, mitral regurgitation; AV, aortic valve; MV, mitral valve. Scale bars: 100 μm. (**B**) Representative double-immunofluorescence stained sections for periostin (green) and vWF (red) are shown. The boxed regions are shown at higher magnification in the right panels. Periostin expression is specifically increased in the areas of neoangiogenesis in atherosclerotic AS. Scale bars: 500 μm (100 μm for the higher magnification).

Supplementary Figure 5

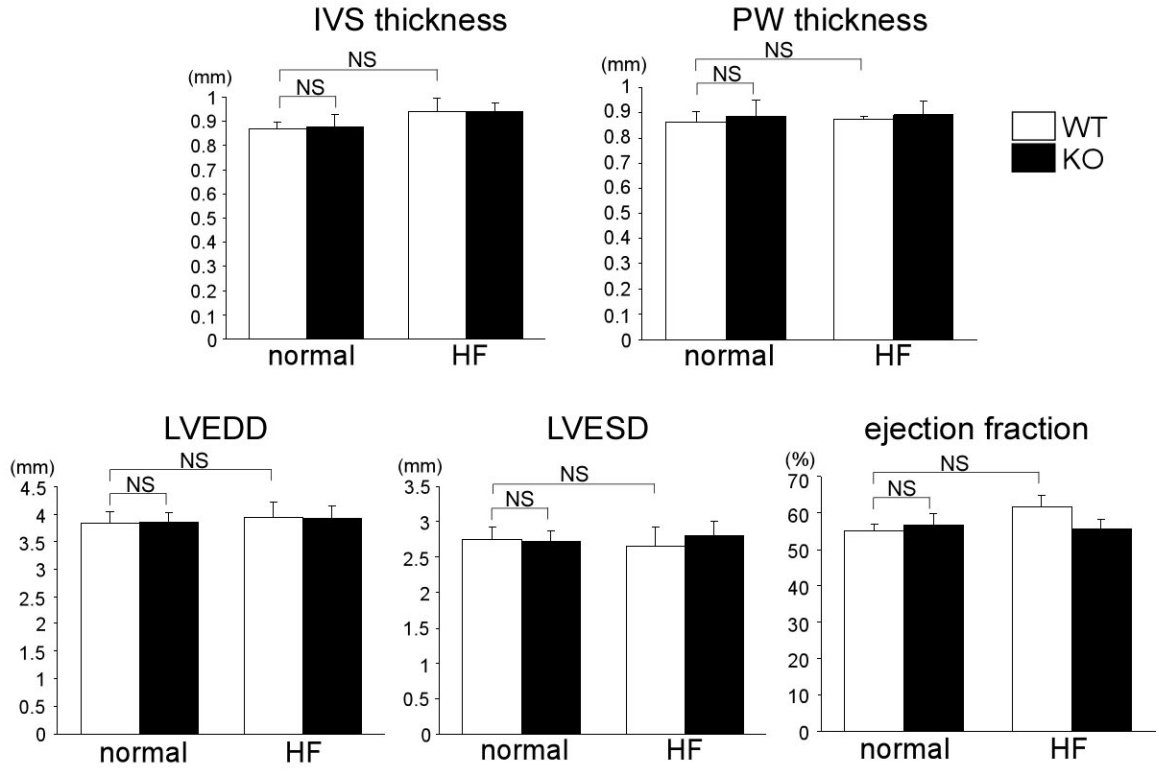

Wall thickness, diameter, and systolic function of the LV are not affected in *Periostin* KO mice. The various parameters of the LV were analyzed in the M-mode of the left parasternal short axis view of echocardiography. IVS, interventricular septum; PW, posterior wall; LVEDD, LV end diastolic diameter; LVESD, LV end systolic diameter; NS, not significant.

Supplementary Figure 6

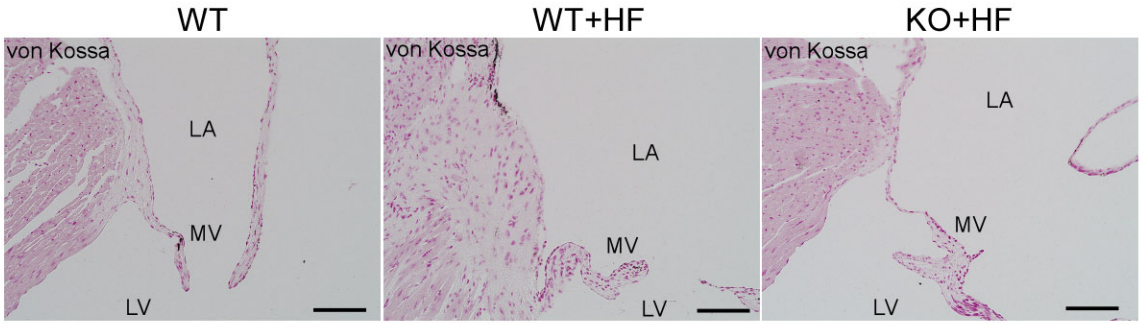

The HF diet induces modest calcification of the mitral valve annuli in the WT mice. Representative sections with von Kossa staining of the mitral valve annuli of the WT and *Periostin* KO mice. Scale bars: 100 μm.

Supplementary Figure 7

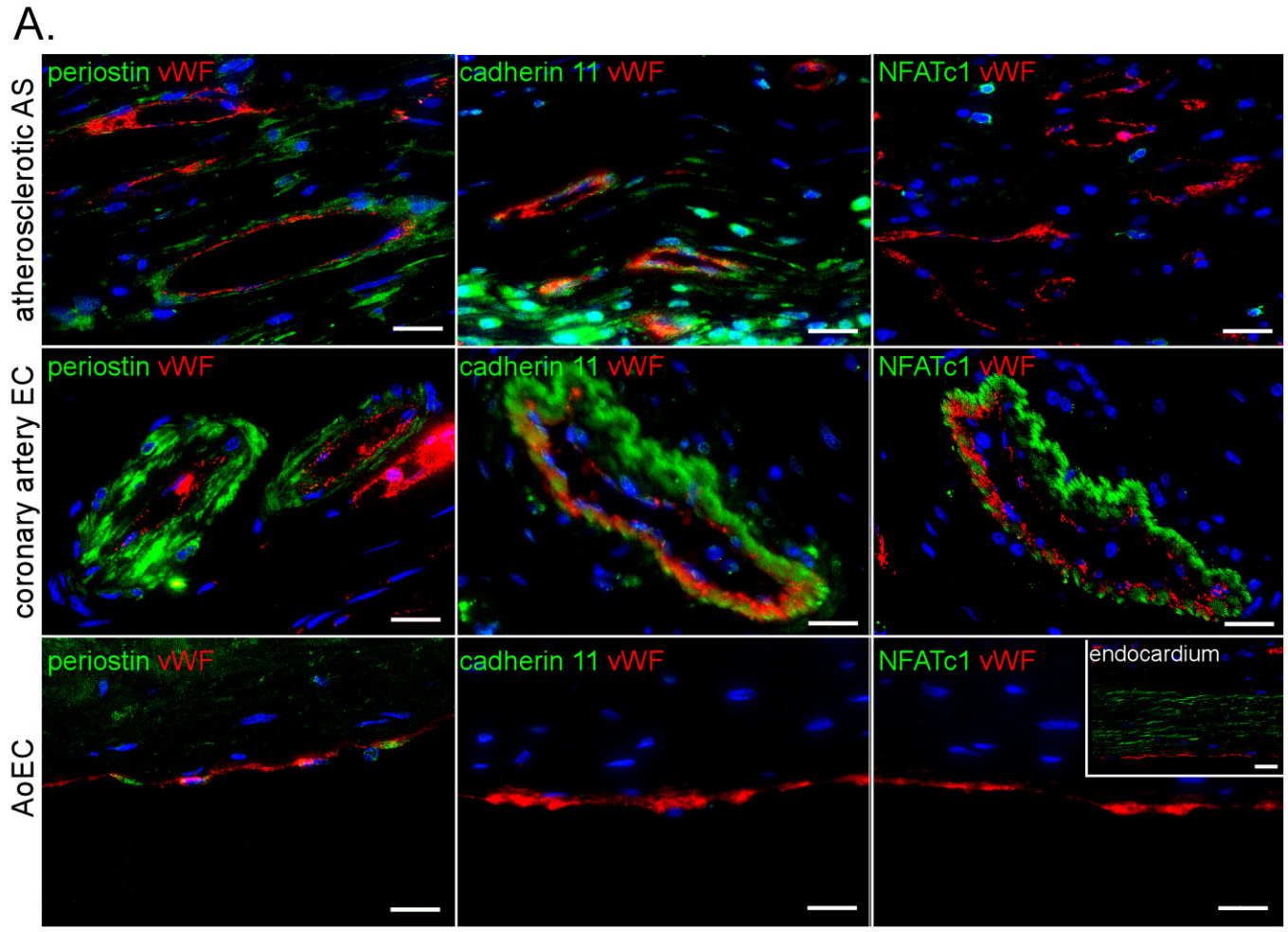

The phenotype of human coronary artery ECs. **(A)** Triple-immunofluorescence staining for vWF (red) and periostin, cadherin 11, and NFATc1 (green) in the ECs located in areas of neoangiogenesis in atherosclerotic AS, human coronary artery ECs, and aortic ECs. Nuclei are stained blue. Endocardium is used as a positive control for NFATc1 expression. Note that cadherin 11, but not periostin, is expressed in the coronary artery ECs, as well as in the ECs in AS, whereas periostin, but not cadherin 11, is expressed in the aortic ECs. Therefore, the phenotype of coronary artery ECs differs from that of aortic ECs. NFAT, nuclear factor of activated T cells; AS, aortic valve stenosis; AoEC, aortic ECs. Scale bars: 20 μm. **(B)** Western blot analysis of the expression of periostin and cadherin 11 in cultured human coronary artery ECs *in vitro*. MC3T3-E1 is used as a positive control for the expression of periostin and cadherin 11.

Supplementary Figure 8

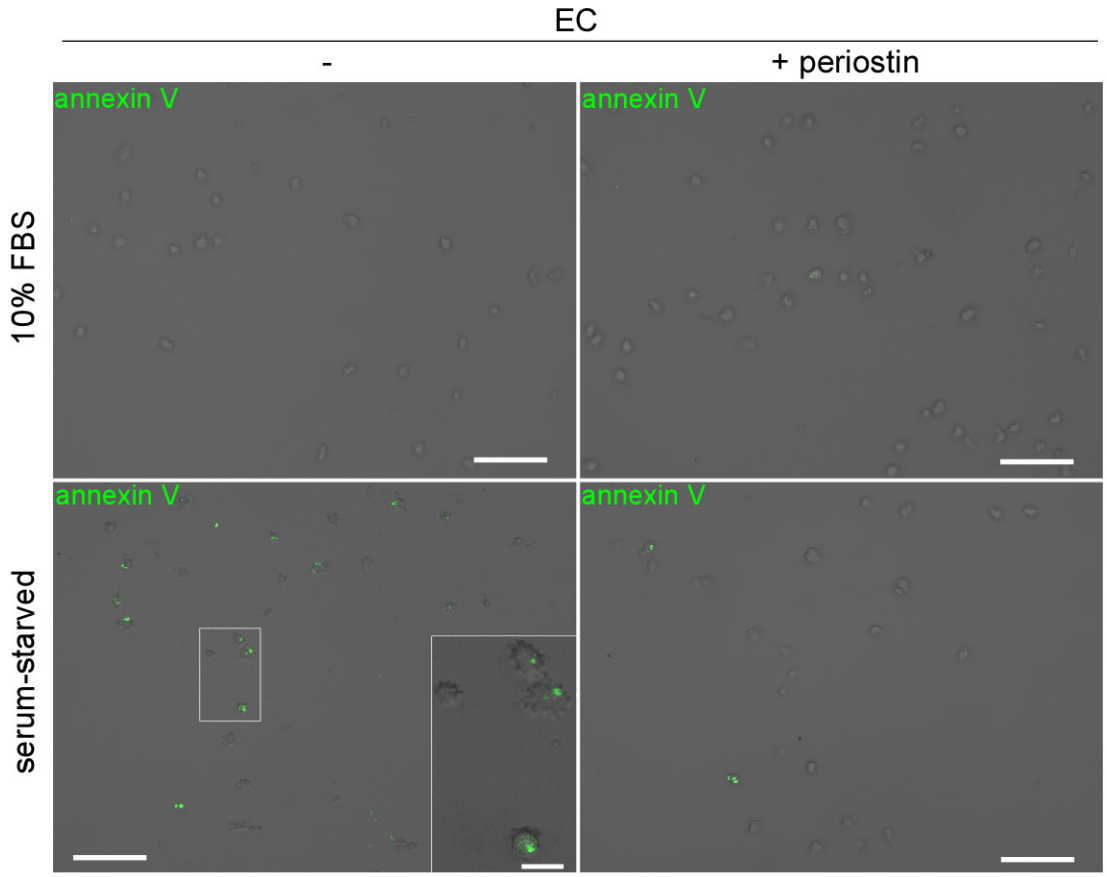

Periostin inhibits serum starvation-induced EC apoptosis *in vitro*. The merged images of annexin V immunofluorescence (green) and a phase-contrast image of the EC are presented. The boxed region is shown at higher magnification in the inset. Scale bars: 100 μm (20 μm for higher magnification).

Supplementary Figure 9

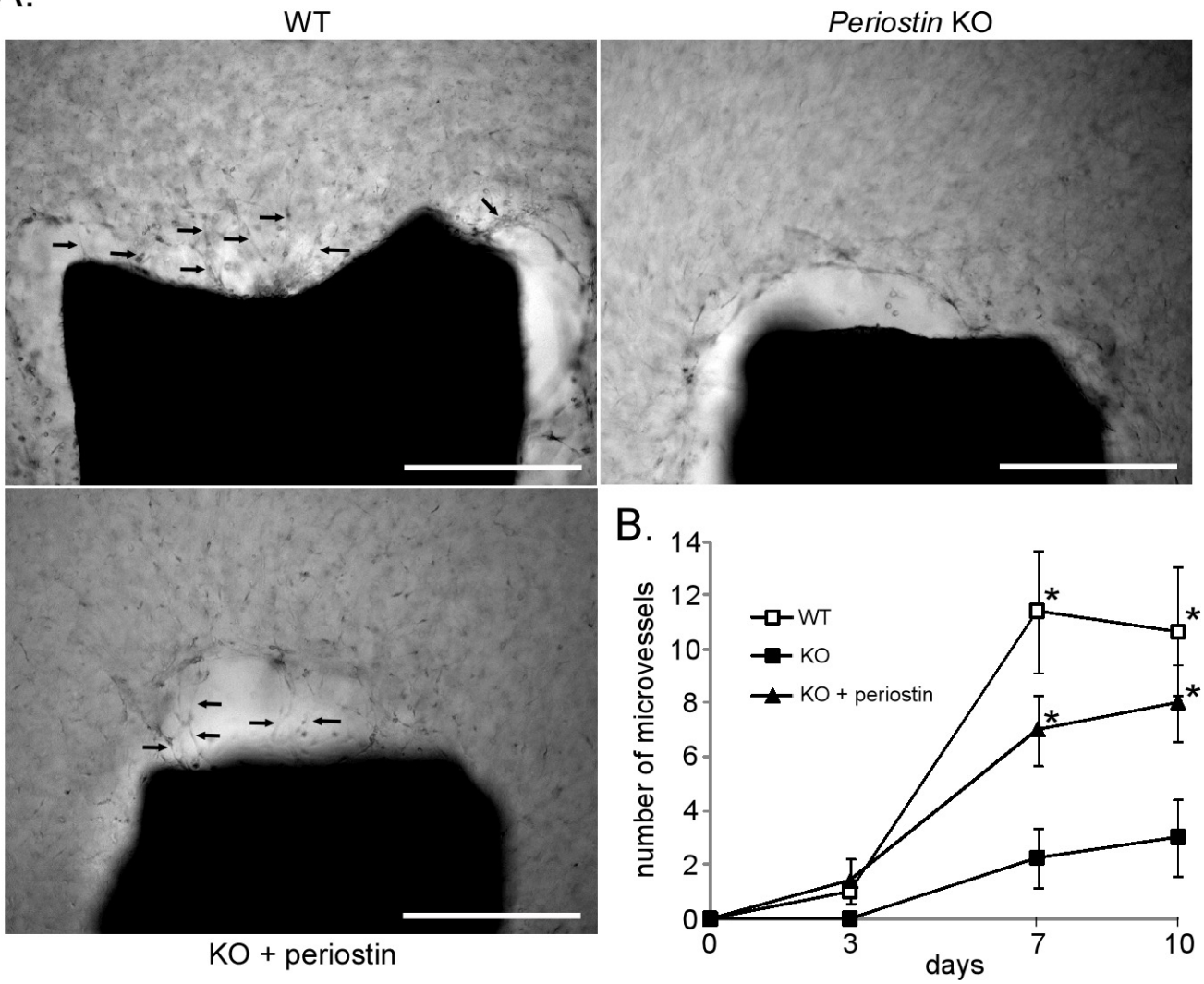

Ex vivo aortic ring angiogenesis assay for WT and *Periostin* KO mice. **(A)** Representative phase-contrast images of mouse aortic roots in collagen gel cultures on Day 7, with or without supplementation with recombinant periostin protein. Microvessels that radiate outwards are indicated by arrows. Scale bars: 100 μm. **(B)** Temporal quantitative analysis of angiogenesis in the aortic ring assay. Periostin strongly promotes *ex vivo* angiogenesis in the murine aortic root. **P* < 0.05 vs. KO.

Supplementary Figure 10

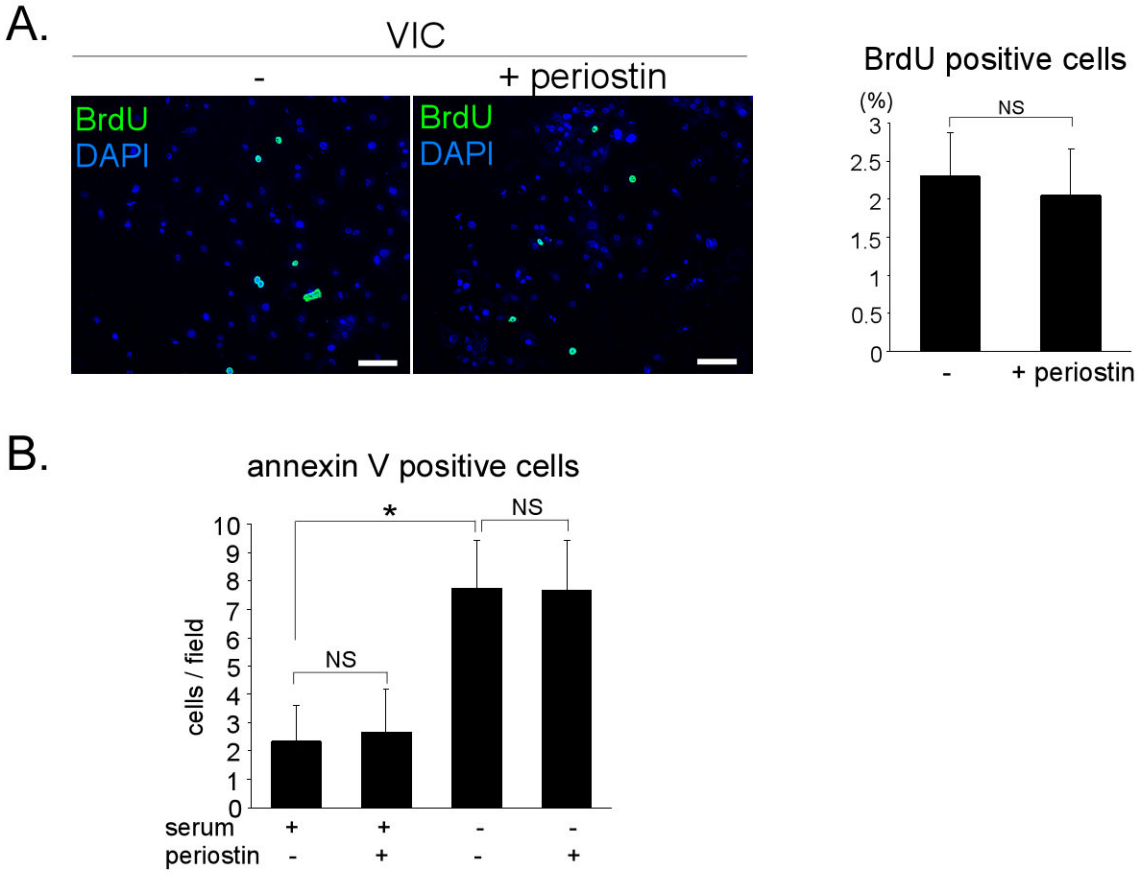

Periostin affects neither the proliferation nor the apoptosis of VICs. (**A**) BrdU incorporation assay for VICs in the presence or absence of periostin stimulation. Scale bars: 100 μm. (**B**) Apoptosis assay for VICs. The VICs were stimulated for 48 h, as described in Figure 7F. **P* < 0.05.

Supplementary Figure 11

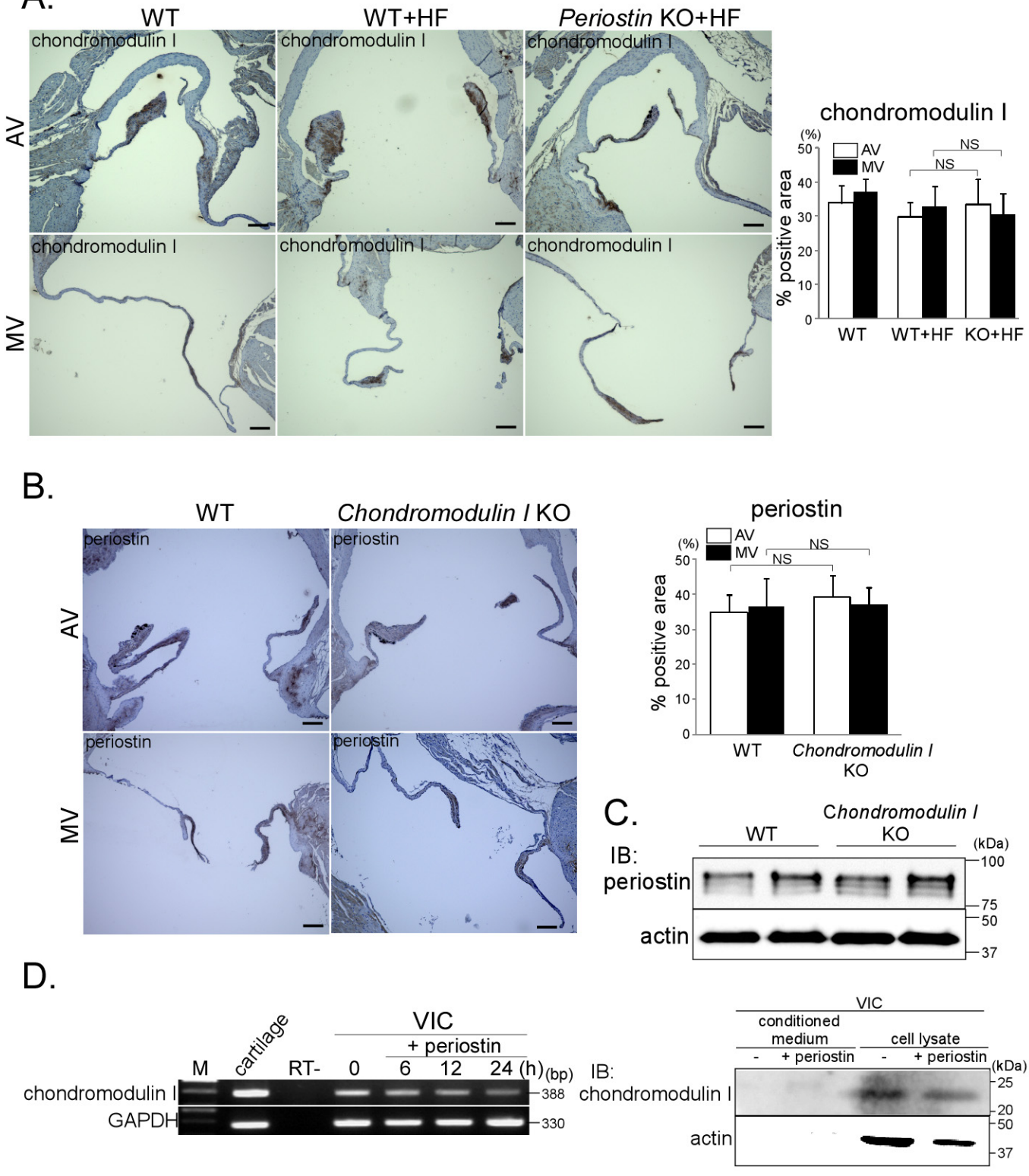

Periostin and chondromodulin I do not cross-regulate each other in murine cardiac valves. (**A**) Representative IHC sections and quantitative analyses of chondromodulin I expression area in the aortic (open bars) and mitral (filled bars) valves of the WT, WT + HF, and *Periostin* KO + HF mice. There is no significant difference in chondromodulin I expression in the valves between HF-fed WT and *Periostin* KO mice. (**B** and **C**) Periostin expression in the WT and *Chondromodulin I* KO mice. Representative IHC sections and quantitative analyses of the expression areas (**B**) and Western blot analysis (**C**) of periostin in the cardiac valves. In **C**, mitral valves with annuli were excised from the mice and subjected to Western blot analysis. The periostin expression levels in the valves of the WT and *Chondromodulin I* KO mice are not different. (**D**) RT-PCR (left) and Western blot (right) analyses of chondromodulin I expression in cultured rat VICs subjected to periostin stimulation. For the Western blot analysis, the VICs were stimulated with or without recombinant human periostin for 5 d, and the conditioned media and cell lysates were collected. Cartilage is used as a positive control for chondromodulin I expression. Scale bars: 100 μm.